ELSEVIER

International Journal of Mass Spectrometry 218 (2002) 173–180

International Journal of Mass Spectrometry

www.elsevier.com/locate/ijms

Secondary ions produced by 400 eV He^+ ion impact on solid films composed of binary mixtures of Ar/Xe, Ar/N_2, and Ar/O_2 at 7 K

K. Hiraoka*, R. Hamamoto, K. Mori, M. Watanabe, T. Sato

Clean Energy Research Center, Yamanashi University, Takeda-4, Kofu 400-8511, Japan

Received 18 January 2002; accepted 30 April 2002

Abstract

Secondary ions produced by 400 eV He^+ ion impact on van der Waals thin films of two-component mixtures of Ar/Xe, Ar/N_2, or Ar/O_2 deposited on a silicon substrate at 7 K were measured as a function of mixing ratio with a film thickness of 100 monolayers using a home-made time-of-flight (TOF) secondary ion mass spectrometer. With an addition of Ar in Xe matrix, a drastic enhancement of Ar^+ was observed. This may be due to the charge transfer reaction, $Xe^{2+} + Ar = Xe^+ + Ar^+$, taking place near the surface of the film. With an addition of Xe in Ar matrix, drastic increases of both Xe^+ and Ar^+ ions were observed. This is due to the trap of holes and excitons by the seeded Xe atoms in Ar matrix resulting in the heavier erosion of the solid film. For Ar/N_2 system, the $N_n{}^+$ ($n = 1$–3) ions show maxima with $Ar/N_2 = \sim 50/50$. This may be due to the shorter diffusion lengths of electronic excitations in this mixing ratio resulting in the heavy erosion of the film near the surface. In contrast, $O_n{}^+$ ($n = 1$ and 2) for Ar/O_2 system show minima with the relative concentration of O_2 in the range 20–80%. This is due to the efficient trap of holes and electrons by the seeded O_2 molecules in the Ar matrix. (Int J Mass Spectrom 218 (2002) 173–180)

Keywords: Secondary ions; Ion impact; Solid films; Binary mixtures

1. Introduction

Despite the wealth of investigation on the reactions of free ions and cluster ions with gas phase molecules, studies on the reactions between the ions and neutral clusters are scarce. This is mainly due to the fact that the method for the formation of size-selected neutral clusters with high intensities is not yet established. In the present work, the interaction between low-energy ions and van der Waals thin films is investigated using a home-made time-of-flight (TOF) secondary ion mass spectrometer. Here the van der Waals thin film deposited on a silicon substrate is regarded as a two-dimensional neutral cluster. The main objective of the current work is to obtain information on the many-body effect on the collision between the low-energy ions and van der Waals solids composed of binary mixtures under the precise control of the film thickness. With the "reactions" of 400 eV He^+ ions with mixed "neutral clusters" of Ar/Xe, Ar/N_2, and Ar/O_2, a unique "cooperative effect" for the formation of secondary ions was observed.

The sputtering of solidified gases has been investigated by a number of groups. The challenge in this field has been to identify the mechanism behind the sputtering process [1–4]. Sputtering of surfaces of

* Corresponding author. E-mail: hiraoka@ab11.yamanashi.ac.jp

1387-3806/02/$ – see front matter
PII S1387-3806(02)00691-7

condensed gases plays an important role in astrophysical problems [5]. The secondary ion mass spectrometry (SIMS) of rare gas and small-molecule solids has been investigated [6–12]. High yields of cluster ions were observed when the van der Waals solid films were bombarded by the rare gas ions larger than He^+. For He^+, the SIMS spectra obtained were found to be simpler, i.e., the intensities of cluster ions became much weaker. This is due to the fact that the energetic He^+ ion induces mainly local elastic collisions and electronic excitation (and ionization) in solids whereas larger rare gas ion bombardment accompanies the momentum transfer to the target, resulting in the shock wave generation (cohesive motion of solid). Thus, by using the incident He^+ ion, the clearer information on the mechanisms of secondary ion formation can be obtained which is mainly governed by the local elastic collisions and electronic excitations.

SIMS has established a place for itself among analytical techniques largely due to its high sensitivity. In organic SIMS, samples are dissolved in some suitable matrices. This is also the case for matrix-assisted laser desorption mass spectrometry (MALDI). The energy transferred to the matrix by the fast particles or by the laser irradiation generates the shock wave in the matrix and the resulting explosive vaporization of the matrix accompanies desorption of the seeded organic molecular ions into the vacuum. Although SIMS has widely accepted in the analytical chemistry, the detailed investigation on the energy relaxation mechanisms of the incident fast particles in the condensed phase has been left largely intact.

In the previous investigations of the SIMS of van der Waals solid films [6–12], the detailed analysis of the roles of holes and excitons for the formation of secondary ions has not been made explicitly albeit it is the main topic in the field of desorption induced by the electronic transition (DIET) [13]. In this work, van der Waals solid films composed of two components were adapted in order to investigate information of the relaxation of electronic excitations (e.g., holes and excitons) to translational energy for the formation of secondary ions. For this purpose, the primary incident ion He^+ may be the best choice because it induces the smallest cohesive momentum transfer in solids among rare gas ions due to its lightest mass.

2. Experimental

The experiments were performed with a home-made TOF secondary ion mass spectrometer which has been described previously [14]. Briefly, a TOF technique is adopted, both for selection of ion species of incident pulsed ion beam and identification of the secondary ions produced from the condensed gas layers. The analyzer system is housed in an ultra-high vacuum (UHV) chamber with a base pressure of 8×10^{-9} Pa. The UHV pumping system consists of a tandem turbo molecular pump and a cryopump.

The substrate for the deposition of the solid film is made of a silicon wafer firmly pressed onto a cold head of a closed-cycle refrigerator. The silicon substrate is electrically insulated using a 0.8 mm thick thermally conductive sheet. The temperature of the substrate is monitored by a chromel vs. Au + 0.07% Fe thermocouple and thermostatted by using a temperature regulator. Sample gas is passed though a molecular sieve (1/1 mixture of 3 and 5 Å) trap kept at liquid nitrogen temperature (for Ar, N_2, and O_2) or at dry-ice acetone temperature (for Xe) at a few 100 Pa and then is deposited on the substrate at 7 K while keeping the sample gas pressure in the range of 10^{-6}–10^{-5} Pa using a variable leak valve. The sticking probability for all species on the cold substrate at 7 K is sufficiently high that as-grown film component was expected to be the same as that in the manifold, which is accurately known based on the partial pressure in the manifold.

In this experiment, about 2×10^7 He^+ ions cm^{-2} were irradiated on the sample film (1.5×10^4 ion pulses) for one mass spectrum acquisition. The reagent He gas (UHP grade, 99.99999%, Iwatani, Kofu) is purified by passing it though a liquid nitrogen cooled molecular sieve 3 Å trap and then is introduced into the ion gun (USC-5, ULVAC-PHI, Kanagawa, Japan). The pressure of He in the vacuum chamber during the operation is $\sim 2 \times 10^{-6}$ Pa. If one assumes a sputtering

rate of 10^2 molecules per ion, it takes about 5×10^5 s to sputter one monolayer (ML) of the film under the present experimental conditions. The collection time for the acquisition of one mass spectrum was about 2×10^2 s. Thus the damage to the film may be totally negligible.

3. Results and discussion

3.1. Xenon/argon system

Fig. 1 shows the relationship between the secondary ion intensities and the mixing ratio for the 100 ML thick film composed of two components of Ar and Xe. All the observed ions show characteristic dependences on the change of the mixing ratio. With an addition of Ar in Xe matrix, sharp increase and decrease in Ar^+ and Xe^+, respectively, are observed. In the separate experiment, a sharp decrease of Xe^+ was also observed when small amounts (less than a few percent) of other rare gases or polyatomic molecules such as N_2, CO, O_2, and CH_4 were added in the neat Xe matrix. This clearly indicates that the intensity of Xe^+ is impurity-sensitive.

The light incident He^+ ion induces electronic excitations, i.e., the formation of holes, electrons and excitons in solids [13]. The charges migrate in solid and finally an atomic ion will bind with the neighboring atom forming the self-trapped molecular ion $R_{g2}{}^+$ in about 10^{-12} s [13]. By the recombination of a self-trapped molecular ion and an electron, a vibrationally hot excimer forms. A transition of the excimer to a repulsive state occurs. Thus the exciton $R_g{}^*$ is formed with kinetic energy. The energy released in this event is 1–2 eV. The $R_g{}^*$ exciton produced can bind with another atom after migration in solid, forming the molecular exciton $R_{g2}{}^*$, which is generally formed in a high vibrational state. The heat is again released to the lattice by the relaxation of this vibrational energy. It is known that the diffusion lengths of holes and excitons in rare gas solids are of the order of 10^2–10^3 Å [15]. By the addition of Ar in the Xe matrix, the periodicity of the lattice is disturbed and the diffusion of holes and excitons in solid may be suppressed. The observed sharp decrease in the intensity of Xe^+ with increase of the relative concentration(C) of C(Ar) = 0 → 10% strongly suggests that the holes and excitons play important roles for the formation of the secondary ion Xe^+ for the pure Xe matrix as already

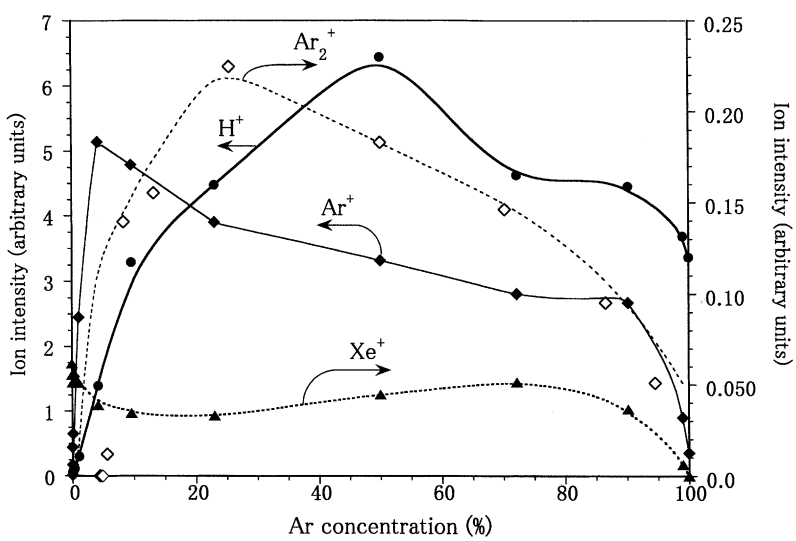

Fig. 1. The relationship between the secondary ion intensities and the mixing ratio for the 100 ML thick film composed of two components of Ar and Xe. Temperature of the film is 7 K.

mentioned earlier. Because the diffusion length of the electronic energies becomes limited by the addition of the Ar impurity, a smaller number of Xe^+ ions can escape into the vacuum compared to the case for the neat Xe matrix in which the excitation of translational energy ranges in a wider region and more Xe^+ ions along the track of the incident He atom can be ejected into the vacuum.

A sudden increase of Ar^+ at the expense of Xe^+ with an addition of a few percent of Ar in Xe in Fig. 1 is interesting because the ionization energy of Ar (15.8 eV) is higher than that of Xe (12.1 eV) and the ionization of Ar by the primary Xe^+ in the plume is unlikely. The direct ionization of the seeded Ar by the incident He^+ is also unlikely because the low concentration of Ar in Xe matrix does not explain the strong appearance of Ar^+ at only a few percent of Ar in Fig. 1. As was reported in our recent work [16], the doubly charged ion Xe^{2+} was produced from the neat Xe solid film bombarded by the 400 eV He^+. Michl and coworkers [11] also found that the solid Ar matrix yields Ar^{2+} with the He^+ and Ne^+ bombardment, and the solid Kr and Xe matrices yield Kr^{2+} and Xe^{2+}, respectively, with He^+, Ne^+, and Ar^+ bombardment. They interpreted the formation of Xe^{2+} by the He^+ bombardment as follows. The He^+ impinging the Xe matrix is neutralized first. Then, He atom collides with Xe atom to sputter three electrons to form Xe^{2+} and He^+. At the moment of the ionic collisions on the surface, a heavy track of the highly ionized plasma is produced and the Coulomb repulsion of the plasma expels the formed doubly charged ions from the surface to the vacuum. During this process, very violent processes take place, i.e., the formation of multiply charged ions, bond dissociation, and heavy electronic excitation. This hot core expands to the environment through the holes and exciton migration, resulting in the release of heat leading the evaporation of the matrix atoms. The evaporated atoms dilute the high-dense ions and carry them to the vacuum as single ions and also cluster ions. The hot ions may be ejected first and this is followed by the cooler gas containing the cluster ions. The evaporation may cease in less than nanoseconds.

We conjecture that the observed selective ionization of Ar in Fig. 1 takes place by the charge transfer reaction (1).

$$Xe^{2+} + Ar = Xe^+ + Ar^+ \quad (1)$$

Some part of Xe^+ may also be produced by the charge transfer reaction (2) in which the doubly charged ion also takes part in.

$$Xe^{2+} + Xe = Xe^+ + Xe^+ \quad (2)$$

The occurrence of reaction (1) suppresses that of reaction (2) with increase of C(Ar) in Fig. 1. The rate constant of reaction (1) measured in the gas phase was reported to be 4×10^{-10} $cm^3\,s^{-1}$ [17] which is smaller than the Langevin collision rate ($\sim 10^{-9}$ $cm^3\,s^{-1}$). The charge transfer reactions involving the multiply charged ions such as reactions (1) and (2) generally have the activation energy, because the intermediate complexes (e.g., $[Xe^+ \cdots Ar^+]^*$) experience the strong Coulomb repulsion along the repulsive potential surface. The internal energy released as a kinetic energy for the falling-apart intermediate complex $[Xe^+ \cdots Ar^+]^*$ is mainly donated to the lighter Ar^+ than the heavier Xe^+. The kinetic energy donated to Ar^+ helps its desorption into the vacuum resulting in the higher sensitivity for Ar^+ than for Xe^+. The observed decrease in Ar^+ with C(Ar) > 5% may be due to the occurrence of the resonant charge transfer reaction (3) (annihilation of the energetic Ar^+) and/or the clustering reaction (4) with increase of the Ar content, and also due to the decrease in the Xe^{2+} ion formation.

$$Ar^+ (\text{fast}) + Ar (\text{slow}) = Ar (\text{fast}) + Ar^+ (\text{slow}) \quad (3)$$

$$Ar^+ + Ar + M = Ar_2^+ + M \quad (M : \text{third body}) \quad (4)$$

Rapid increases in Xe^+ and Ar^+ are observed in Fig. 1 when a small amount of Xe is added to the Ar matrix. The enhancement of Ar^+ by the addition of Xe impurity must be due to the efficient trap of holes and excitons by the seeded Xe atoms in the Ar matrix. The energy trapped and localized in the Xe atoms may lead to the formation of hot high-pressure plume confined near the surface of the film. This enhances the desorption of Ar^+ and also Xe^+ formed along the

track of the incident He atom into the vacuum. The intensity of Xe^+ reaches the maximum with C(Xe) = 30%. This suggests that the energy of the incident He^+ ion is most efficiently converted to the phonon excitation with this concentration.

In Fig. 1, the strong appearance of the H^+ ion is observed. In our previous paper [14], it was suggested that the H^+ ion originates mainly from the silicon substrate whose surface is terminated by Si–H bonds by the chemical etching using hydrofluoric acid. The persistent appearance of H^+ with increase of film thickness ≥100 ML for N_2, Ar, and Kr also suggests that the appearance of H^+ is due to impurities of hydrogenated compounds (e.g., H_2O, H_2, hydrocarbons, etc.) in the film [16]. In the current work, a considerable effort was made to eliminate impurities in the sample gases introduced in the vacuum chamber. However, the H^+ ion persists to appear with a strong intensity. At present, the mechanisms for the formation of strong H^+ is not well understood.

In Fig. 1, the intensity of the impurity-origin H^+ ion is relatively weak for the neat Xe film. This is because the ionization potential of H (13.6 eV) is higher than that of Xe (12.1 eV) and, thus, the charge transfer reaction, $Xe^+ + H = H^+ + Xe$, is endothermic. The rapid increase in H^+ with increase of Ar concentration can be reasonably explained by the charge transfer reaction, $Ar^+ + H = H^+ + Ar$.

3.2. Argon/nitrogen system

Fig. 2 shows the intensities of ions as a function of mixing ratio for the Ar/N_2 system. With an addition of N_2 in the Ar matrix up to $C(N_2) = 10\%$, a drastic decrease in the Ar^+ intensity is observed. It is evident that the desorption of Ar^+ for the neat solid argon is greatly suppressed by the addition of N_2. This must be due to the efficient trap of holes (Ar^+) and excitons by the seeded N_2 molecules in the Ar matrix. This is reasonable because the ionization energy of gas phase N_2 (15.6 eV) is slightly lower than that of Ar (15.8 eV).

With $C(N_2) \geq 10\%$, the intensity of Ar^+ decreases almost linearly with decrease of Ar content. In the range of C(Ar) = 0–90%, the Ar^+ intensity is approximately proportional to the relative concentration of Ar. This suggests that the Ar^+ ions are formed near the top surface of the sample film mainly by the linear cascade regime [18] and that desorption of Ar^+

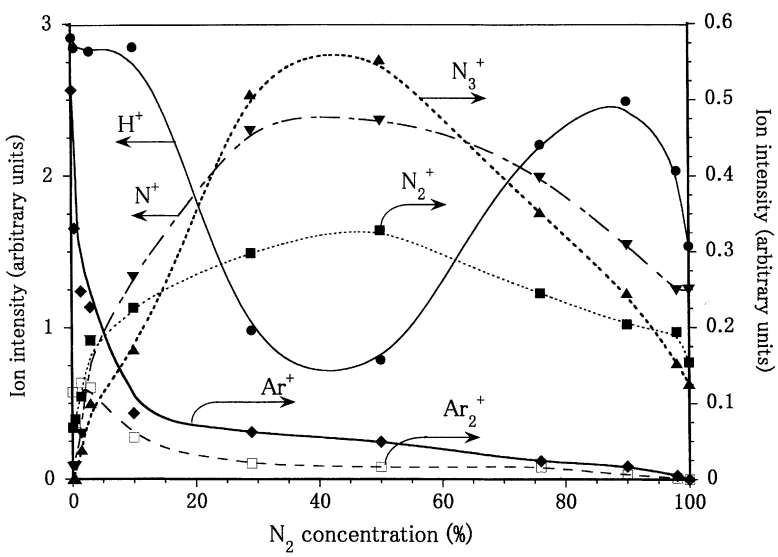

Fig. 2. The relationship between the secondary ion intensities and the mixing ratio for the 100 ML thick film composed of two components of Ar and N_2. Temperature of the film is 7 K.

by the spike regime [18] is minor in this concentration range. Such an event must occur in the early stage of the cascade collisions (i.e., knock-on and linear cascade regime [18]) in the range of 10^{-14}–10^{-13} s (time required for the escape from the place of birth to the vacuum with the kinetic energy of a few electron volts) without the participation of the spike regime [18]. In contrast, the greater part of Ar^+ observed in $C(N_2) = 0$–5% is attributed to those assisted by the spike regime [18], i.e., the slower events in the range of 10^{-12}–10^{-9} s. From the extrapolated value of the linear portion of the Ar^+ ion intensity to $C(Ar) = 100\%$, one may predict that the ions produced by the slower events (spike regime) are about four times larger than those produced by the more direct early events (the single knock-on and the linear cascade regime).

A small addition of N_2 into the Ar matrix leads to the strong growths of ions originating from the seeded N_2, i.e., N^+, $N_2{}^+$, and $N_3{}^+$ in Fig. 2. This is also due to the efficient trap of holes and excitons by the seeded N_2 molecules followed by the degradation to the translational energy. Because the N_2 molecule has much larger density of states of rovibronic energy levels than the Ar atom, the electronic excitation energies imparted in solid must be quickly transferred to the impurity N_2 molecules. This explains the marked sensitization of the N_2-originating ions by the addition of N_2 in the Ar matrix in Fig. 2.

The ratio of the intensities of $N_3{}^+$ and N^+, $I(N_3{}^+)/I(N^+)$, becomes largest at about $C(N_2) = 50\%$. This suggests that the N^+ ion has the greatest chance to collide with the N_2 molecules to form the associated ion $N_3{}^+$ at this concentration. That is, the plume produced in this mixing ratio is such that the clustering reaction (5) proceeds efficiently and at the same time the produced ions are efficiently entrained in the effusing plume into the vacuum (i.e., the formation of rather dense and hot plume).

$$N^+ + N_2 + M = N_3{}^+ + M \quad (M : \text{third body}) \qquad (5)$$

In our previous work [14], it was found that the intensities of N^+ and $N_3{}^+$ produced by the 400 eV He^+ impact on the N_2 solid film deposited on the silicon substrate reached the plateau with the film thickness of only 5 ML. This indicates that the spike region for the formation of secondary ions is unexpectedly thin (≈5 ML). This may be due the fact that the holes, electrons, and excitons have long diffusion lengths in N_2 solid and the hole–electron recombination takes place far apart to each other and, thus, it does not lead to the heavy sputtering in the N_2 solid in the extended region. Since the lowest triplet sate of $N_2(^3\Sigma_u^+)$ has a long lifetime, we think that the efficient triplet–exciton migration in the N_2 solid takes place (i.e., the Dexter mechanism). In the recombination of holes ($N_2{}^+$) and electrons, the probability for the formation of triplet states is three times larger than that of the singlet states. In the gas phase, the $N_2(^3\Sigma_u^+)$ state is about 6 eV above the ground state. We guess that some part of the internal energy imparted to the N_2 film (e.g., $N_2(^3\Sigma_u^+)$ triplet exciton) may be dissipated to the silicon substrate which acts as a perfect energy sink [19]. This explains the shallow spike region observed for the neat N_2 film, resulting in the weak intensities for $N_n{}^+$ ($n = 1$–3) ions in Fig. 2.

3.3. Argon/oxygen system

Fig. 3 displays the relationship between the intensities of ions and the mixing ratio for the Ar/O_2 system. There are many characteristic differences between Figs. 2 and 3. After a small but sharp decrease, the Ar^+ ion shows only a gradual decrease keeping its rather strong intensity in the range of $C(O_2) = 5$–90% and decreases sharply to 0 with $C(O_2) = 90$–100%. The decrease of Ar^+ with an addition of O_2 in the neat Ar matrix clearly indicates that the holes (Ar^+) are trapped by the seeded O_2 molecules in the solid sample. However, in contrast to the case of the Ar/N_2 system, a relatively strong Ar^+ signal persists to appear in the wide range of $C(O_2) = 2$–90%. It is evident that the efficient desorption of Ar^+ due to the spike regime takes place in the mixed O_2/Ar solid. That is, the electronic excitations in the solid of Ar/O_2 mixture are efficiently converted to the translational energy and an extended plume is generated for the desorption of ions. This is a marked contrast to the fact that the conversion of holes and excitons to

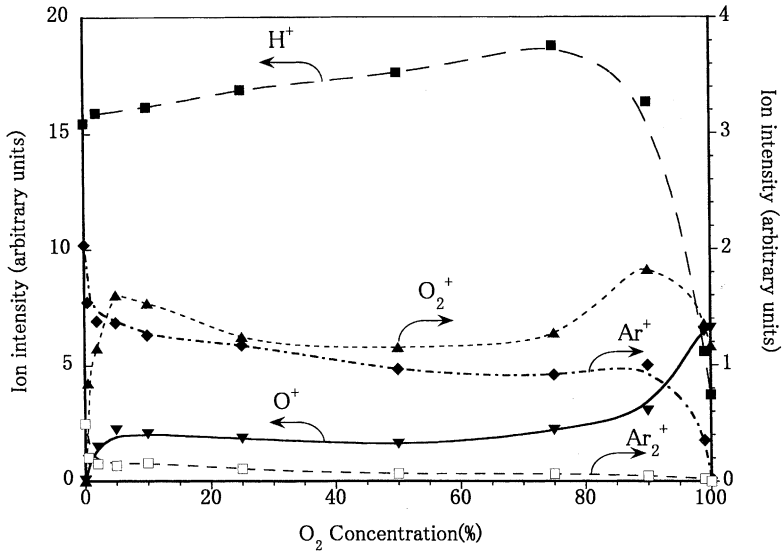

Fig. 3. The relationship between the secondary ion intensities and the mixing ratio for the 100 ML thick film composed of two components of Ar and O_2. Temperature of the film is 7 K.

the translational energy is much less efficient in the Ar/N_2 system. The observed efficient relaxation of the electronic energies to the translational energy in the Ar/O_2 solid film must be due to the efficient recombination of holes and electrons and/or to the short diffusion lengths of electrons, holes, and excitons in solids. Because the gas phase electron affinity of O_2 is positive (0.44 eV) [20], the electron in solid O_2 may be easily trapped as a negative ion as O_2^-. The thermochemical stability of gas phase cluster ions of $O_2^-(O_2)_n$ has been measured with a high-pressure mass spectrometer [21]. It was found that the nature of bonding in $O_2^-(O_2)_n$ changes drastically from covalent to electrostatic between $n = 1$ and 2. That is, the core ion in the cluster is $(O_2)_2^-$ and the cluster ion can be represented as $(O_2)_2^-(O_2)_{n-1}$ [21]. The trapped electrons in the solid O_2 may exist as the O_4^- ion interacting with surrounding O_2 ligands by the weak electrostatic force. The formed trapped electrons as O_4^- will recombine with the mobile holes leading to the film erosion. Because the rate constant of the charge transfer reaction (6) is small (5×10^{-11} cm^3 molecule^{-1} s^{-1}) [22], the Ar^+ ion may have enough chance to survive in the plume to be detected as secondary ions.

$$Ar^+ + O_2 = O_2^+ + Ar \quad (6)$$

This explains the biased intense Ar^+ in the range of $C(O_2) = 2$–90% in Fig. 3.

By an addition of O_2 in a neat Ar matrix, sharp increases of O^+ and O_2^+ are observed in Fig. 3. More efficient relaxation to the translational energy due to the recombination of trapped holes and electrons also explains the enhanced desorption of these secondary ions. When the concentration of O_2 is low, the translational energy may well be extended due to the dispersed O_2 molecules in solid. With increase of the O_2 content, the average distance of trapped positive and negative sites become closer and consequently a size-limited hotter plume may be generated.

When Ar is added in the neat O_2 matrix, increases of O_2^+ and Ar^+ and a decrease of O^+ are observed in Fig. 3. The fast He atom injection in the solid O_2 generates electronically excited molecules and ions that dissociate to O and O^+ (e.g., Schumann–Runge transition). In the collision of the incident He with target molecules in condensed phases, significant overlap

of the molecular orbitals of the target and the atomic orbitals of the projectile He atom can occur. By the addition of Ar in the molecular O_2 solid, a fraction of the direct electronic excitation of O_2 molecules decreases and that for the formation of holes and excitons via the electronic excitations of Ar atoms increase. This explains the increase in O_2^+ and Ar^+ and the decrease in O^+ by the addition of Ar in the O_2 solid in Fig. 3.

The relatively weak H^+ ion observed for the neat O_2 solid in Fig. 3 is understandable because the ionization energy of H (13.6 eV) is higher than that of O_2 (12.3 eV) and the ionization of H atoms by the O_2^+ ions is energetically unfavorable. The charge transfer reaction, $Ar^+ + H = H^+ + Ar$, taking place in the plume leads to the sharp increase in H^+ by the addition of Ar in the O_2 matrix. The strong appearance of H^+ is observed in all Figs. 1–3. The fact that the components that give the strong ion signal of H^+ are not the major ones but the hydrogen-containing impurities clearly manifests the complexity of the secondary ion formation. Much more effort must be made to clarify the mechanisms for the formation of secondary ions. Variation of the energy and nature of the primary ion, film thickness dependence, use of isotopes, and the estimate of the sputtering yield should be our next projects.

References

[1] O. Ellegaard, J. Schou, H. Sørensen, P. Børgesen, Surf. Sci. 167 (1986) 474.
[2] W.L. Brown, W.M. Augustyniak, E. Brody, B. Cooper, L.J. Lanzerotti, A. Ramirez, R. Evatt, R.E. Johnson, Nucl. Instrum. Methods 170 (1980) 321.
[3] W.L. Brown, W.M. Augustyniak, L.J. Lanzerotti, R.E. Johnson, R. Evatt, Phys. Rev. Lett. 45 (1980) 1632.
[4] D.E. David, J. Michl, Prog. Solid State Chem. 19 (1989) 283.
[5] L.J. Lanzerotti, W.L. Brown, R.E. Johnson, Ices in Solar System, in: J. Klinger (Ed.), Reidel, Dordrecht, 1985, p. 317.
[6] F. Honda, G.M. Lancaster, Y. Fukuda, J.W. Rabalais, J. Chem. Phys. 69 (1978) 4931.
[7] H.T. Jonkman, J. Michl, Anal. Chem. 50 (1978) 2078.
[8] G.M. Lancaster, F. Honda, Y. Fukuda, J.W. Rabalais, J. Am. Chem. Soc. 101 (1979) 1951.
[9] M. Barber, J.C. Vickerman, J. Wolstenholme, J. Chem. Soc. Faraday I 76 (1980) 549.
[10] H. Jonkman, J. Michl, J. Am. Chem. Soc. 103 (1981) 733.
[11] R.G. Orth, H.T. Jonkman, D.H. Powell, J. Michl, J. Am. Chem. Soc. 103 (1981) 6026.
[12] R.G. Orth, H.T. Jonkman, J. Michl, J. Am. Chem. Soc. 104 (1982) 1834.
[13] R.E. Johnson, M. Inokuti, Nucl. Instrum. Methods 206 (1983) 289.
[14] T. Sato, A. Shimizu, K. Nakamua, K. Hiraoka, Rapid Commun. Mass Spectrom. 11 (1997) 1139.
[15] M. Runne, G. Zimmerer, Nucl. Instrum. Methods Phys. Res. B 101 (1995) 156.
[16] K. Hiraoka, submitted for publication.
[17] A.A. Viggiano, F. Howorka, J.H. Futrell, J.A. Davidson, I. Dotan, D.L. Albritton, F.C. Fehsenfeld, J. Chem. Phys. 71 (1979) 2734.
[18] G. Bets, K. Wien, Int. J. Mass Spectrom. Ion Processes 140 (1994) 1.
[19] C.T. Reimann, W.L. Brown, R.E. Johnson, Phys. Rev. B 37 (1988) 1455.
[20] R.J. Celotta, R.A. Bennet, J.L. Hall, M.W. Siegel, J. Levins, Phys. Rev. A 6 (1972) 631.
[21] K. Hiraoka, J. Chem. Phys. 89 (1988) 3190.
[22] Y. Ikezoe, S. Matsuoka, M. Takebe, A. Viggiano, Gas Phase Ion-Molecule Reaction Rate Constants Through 1986, 1987, Maruzen, Tokyo.